論 文

Designing Passive-Type Radar Reflector for Small Ship

Jeong-Bin Yim* · Woo-Suk Kim* · Yoeng-Sub Ahn* · Sung-Hyeon Park* · Jung-Sik Jung* · Kyu-Dong Lee**

*Division of Maritime Transportation System, Mokpo National Maritime University, Mokpo, 530-729, Korea

**Graduate School of Mokpo Maritime University, Mokpo 530-729, Korea

임정빈* · 김우숙* · 안영섭* · 박성현* · 정중식* · 이규동**

*목포해양대학교 해상운송시스템학부 교수, **목포해양대학교 대학원 석사과정

〈目 次〉

Abstract

This paper describes on the design of Passive-type Radar Reflector for small Ship (PRR-S) based on the newly revised 2000 SOLAS regulations. The design idea, adopted in the study, is to hold PRR-S in the proper 'catch rain' position to avoid fluctuations of Radar Cross Section (RCS) due to ship's heeling. The PRR-S consists of octahedral-type radar reflector with circular plates and three-axis gimbaled stabilizer with weight on the bottom of outer gimbal ring. Performance test for the PRR is carried out in an anechoic chamber. The test results show that the reflected radar signal from PRR-S is more uniformly distributed than the reference model (Davis Echomaster).

KEY WORDS : SOLAS 2000, Passive-type Radar Reflector, Radar Cross Section(RCS), Gimbaled Stabilizer

요 약

이 논문에서는 새로 개정된 2000 SOLAS 규정에 근거하여 소형선박용 수동식 레이더 리프렉터(PRR-S) 설계에 관해서 기술했다. 이 연구의 설계개념은 PRR-S이 선박요동에 의해서 레이더 반사면적(RCS)이 변동하는 것을 방지하기 위하여 'catch rain' 위치를 유지하도록 한 것이다. PRR-S은 원형판으로 구성한 옥타헤더럴 레이더 리프렉터와 요동방지를 위한 짐발장치로 구성하였다. 설계한 PRR-S는 전파흡수실에서 성능실험을 하였다. 실험결과, 기준으로 정한 Davis Echomaster사의 리프렉터 보다 설계한 PRR-S이 높은 RCS를 나타냈다.

핵심단어 : SOLAS 2000, 수동식 레이더 리프렉터, 레이더 반사면적(RCS), 짐발 안정기

*목포해양대학교 해상운송시스템학부 교수

**목포해양대학교 대학원 석사과정

1. INTRODUCTION

On 14 April 1912, Titanic foundered and safety standards in the shipbuilding changed forever. Soon after the tragedy, the International Maritime Organization (IMO) was established to investigate maritime laws and regulations. The IMO prompted the first Safety Of Life At Sea (SOLAS) conference. SOLAS represented an international agreement to secure the protection of life at sea. Then, the SOLAS chapter V is revised with several relevant resolutions in July 2000. These amendments entered into force on 1 July 2002 [1].

Collision avoidance is surely the most important part at sea traffic. Especially, small and medium sized ship is surprisingly poor targets for radar reflection and is frequently in danger of being overrun by larger vessels, even under good conditions of visibility. Most of the small vessel, with wood and fiberglass hulls, even those with metal masts and engines, do not possess enough reflective qualities to make them highly visible on a radar screen. In addition, small radar reflectors may not show up on a ship as radar, due to rain or background wave clutter. Thus, the IMO suggests that a small ship should carry a radar reflector to assist detection by ships navigating by radar at both 9 and 3 GHz [2],[3].

The classic reflector is made of three planar circles or squares of metal intersecting at right angles, forming eight trihedral reflectors. In the usual 'catch rain' position, one trihedral will face up and one down, and the remaining six are arrayed around a circle, three oriented 18° above the equator, and three 18° below. This optimizes the return from the 'pockets', and avoids the nulls or gaps as best as is possible, but only at a 0° angle of heel [4]~[10].

An essential design feature of a reflector, which greatly enhances the effective amount of signal returned, is the accuracy of the right angles formed between the plates. The proper alignment of one of the angles must be within 3° of a right angle or half of the reflected signal will be lost. Thus, alignment of reflector angle is key factor in reflector performance [11].

With consideration of ship's rolling, pitching and yawing, the best way to keep the 'catch rain' position is of use a heeling protection device, such as three-axis gimbaled stabilizer. This paper presents the development of a new passive-type radar reflector based on the RCS measurement technology of radar targets and three-axis gimbaled mechanism.

2. RELATED REGULATIONS

The sub-committee on Safety of Navigation of IMO held its forty-sixth session from 10 to 14 July 2000. In the sub-committee, made successful conclusion by NAV. 45 of the revision of SOLAS chapter V. The draft revised text had been approved by MSC 72 and circulated in accordance with SOLAS article Ⅷ for consideration and adoption by MSC 73. The revised chapter so that entered into force on 1 July 2002. The related regulations from 1973 to 2000 for a radar reflectors are summarized as follows [12]~[14]:

❖ Annex 20 Draft Amendments to Chapter 13 of the HSC Code, 2000, Chapter 13 Shipborn Navigational Systems and Equipment and Voyage Data Recorder, 13.13 Radar Reflector:

(1) If practicable, craft of 150 tonnage or below shall be provided with a radar reflector, or other means,

(2) to assist detection by ships navigating by radar at both 9 and 3 GHz.

❖ Resolution A.384(X), adopted on 14 November 1977, Performance Standards for Radar Reflectors (SOLAS Ch. Ⅲ, COLEG Rule 6(b)(iv):

(1) The echoing areas specified are those for the frequency of 9.3GHz (wavelength of 3.2cm).

(2) All vessels of less than 100 tons gross tonnage operating in international waters and adjacent coastal areas should, if practicable, be fitted with a radar reflector.

(3) Radar reflector should be of an approved type with an adequate polar diagram in azimuth, and an echoing area:

(i) preferably, of at least 10㎡, mounted at a minimum height of 4m above water level; or

(ii) if this is not practicable, of at least 40㎡, mounted at a minimum height of 2m above water level..

(4) Performance around 360 °azimuth..

(5) The azimuthal polar diagram should be such that the response over a total angle 240 ° is not less than -6dB with reference to the maxima of the main lobes.

❖ Resolution A.277(Ⅷ), adopted on 20 November 1973, Recommendation on Performance Standards for Radar Reflectors:

(1) This clause is same as (1) in the above resolution A.384(Ⅹ).

(2) Small craft should be fitted with radar reflectors.

(3) The other clauses are also same as (3), (4) and (5) in the above resolution A.384(Ⅹ).

In addition, the U.S. Coast Guard is also considered marine radar reflector requirements that would apply to boats operating in waters of the United States. Already, such a requirement is in existence in many other countries such as the United Kingdom, Canada and Germany.

3. RCS CALCULATION

3.1 Radar and Cross-Section

When radar signals are reflected from irregular surfaces, such as buoys, sailboats and runabouts, they will rebound in many directions, leaving only a small portion to be reflected in the direction of the radar observer. Obviously, some standard had to be used in making meaningful comparisons of various reflective surfaces. The term 'effective radar cross-section', referred to as RCS (Radar Cross-Section), has been adopted worldwide in making comparisons of reflective surfaces as shown in Fig. 1 [15],[16].

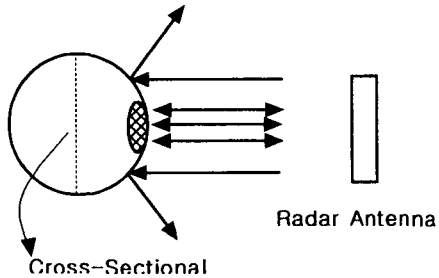

Fig . 1 A metal sphere to indicate Radar Reflector's performance, RCS

In general, marine radar classified into two bands, X-band and S-band. Large vessels will typically carry both, while small vessels are limited to the smaller X-band radar. X-band radar operates at a frequency of approximately 9.4GHz, with a wavelength of 3.2cm, while S-band operates at approximately 3.0GHz, with a longer wavelength of 10.0cm. X-band radar offers greater resolution and detection of smaller targets, but is more susceptible to interference from rain and seas. S-band radar has longer range and less interference from rain and sea clutter, but has less sensitivity for small targets. Thus, the size of reflector will be more large one to get a good performance at both X and S bands.

3.2 RCS Theory

Assume the power density of a wave incident on a target located at rage R away form the radar is P_{Di}. The amount of reflected power from the target is

$$P_r = \sigma P_{Di} \tag{1}$$

σ denotes the target cross section (RCS). Define P_{Dr} as the power density of the scattered waves at the receiving antenna. It follows that

$$P_{Dr} = \frac{P_r}{4\pi R^2} \tag{2}$$

Equating Eqs. (1) and (2) yields

$$\sigma = 4\pi R^2 \left(\frac{P_{Dr}}{P_{Di}}\right) \tag{3}$$

and in order to ensure that the radar receiving

antenna is in the far field, i.e., scattered waves received by the antenna are planar, Eq. (3) is modified

$$\sigma = 4\pi R^2 \lim_{R\to\infty} \left(\frac{P_{Dr}}{P_{Di}}\right) \qquad (4)$$

The RCS defined by Eq. (4) is often referred to as either the monostatic RCS, the backscattered RCS, or simply target RCS. The backscattered RCS is measured from all waves scattered in the direction of the radar and has the same polarization as the receiving antenna. It represents a portion of the total scattered target RCS σ_t, $\sigma_t > \sigma$. Assuming spherical coordinate system defined by (ρ, θ, ϕ), then at range ρ the target scattered cross section is a function of (θ, ϕ). Let the angles (θ_i, ϕ_i) define the direction of propagation of the incident waves. Also, let the angles (θ_s, ϕ_s) define the direction of propagation of the scattered waves. The special case, when $\theta_s = \theta_i$ and $\phi_s = \phi_i$, defines the monostatic RCS. The RCS measured by the radar at angles $\theta_s \neq \theta_i$ and $\phi_s \neq \phi_i$ is called the bistatic RCS. The total target scattered RCS is given by

$$\sigma_t = \frac{1}{4\pi} \int_{\phi_s=0}^{4\pi} \int_{\theta_s=0}^{\pi} \sigma(\theta_s, \phi_s) \sin\theta_s \, d\theta \, d\phi_s \qquad (5)$$

The amount of bacscattered waves from a target is proportional to the ratio of the target size to the wavelength, λ, of the incident waves. In fact, a radar will not be able to detect targets much smaller than its operating wavelength.

The analysis presented in this work assumes far field monostatic RCS measurements in the optical region. Thus, near field RCS, bistatic RCS, and RCS measurements in the Rayleigh region are not be considered. Additionally, RCS treatment in this work is mainly concerned with narrow band cases.

3.3 Analysis of Radar Targets

RCS's for three radar targets[18],[19] are analysed to select the optimum reflection shapes that have high and steady RCS characteristics in heeling angle variation.

Circular Flat Plate

Figure 2 shows a circular flat plate of radius r, centered at the origin. Due to the circular symmetry, the backscattered RCS of a circular flat plat has no dependency on ϕ.

The RCS is only angle dependent. For normal incidence the backscattered RCS for a circular flat plat is

$$\sigma = \frac{4\pi^3 r^4}{\lambda^2}, \quad \theta = 0^0 \qquad (6)$$

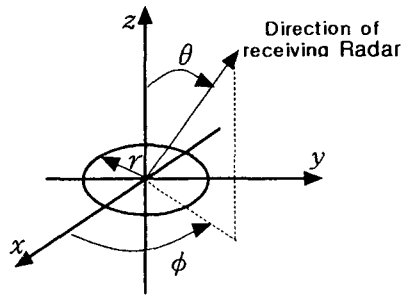

Fig. 2 Coordinates for a circular flat plate

For non-normal incidence, two approximations for the circular flat plate backscattered RCS for any linearly polalized incident wave are

$$\sigma = \frac{\lambda r}{8\pi \sin\theta (\tan\theta)^2}, \quad \theta \neq 0^0 \qquad (7)$$

$$\sigma = \pi k^2 r^4 \left[\frac{2J_1(2kr\sin\theta)^2}{2kr\sin\theta}\right] (\cos\theta)^2, \quad \theta \neq 0^0 \qquad (8)$$

Where $k = \frac{2\pi}{\lambda}$, and $J_1(\beta)$ is the first order spherical Bessel function evaluated at β.

Rectangular Flat Plate

Consider a perfectly conducting rectangular thin plate in the x-y plane as shown in Fig. 3.

The two sides of the plate are denoted by 2a and 2b.

For a linearly polarized incident wave in the x-z plane, the horizontal and vertical backscattered RCS are, respectively, given by

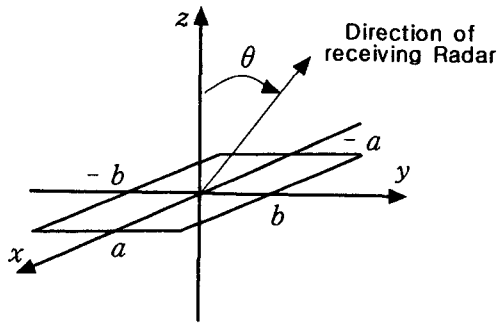

Fig. 3 Coordinates for a rectangular flat plate

$$\sigma_V = \frac{b^2}{\pi}\left|\sigma_{1V} - \sigma_{2V}\left[\frac{1}{\cos\theta} + \frac{\sigma_{2V}}{4}(\sigma_{3V}+\sigma_{4V})\right]\sigma_{5V}^{-1}\right|^2 \quad (9)$$

$$\sigma_H = \frac{b^2}{\pi}\left|\sigma_{1H} - \sigma_{2H}\left[\frac{1}{\cos\theta} + \frac{\sigma_{2H}}{4}(\sigma_{3H}+\sigma_{4H})\right]\sigma_{5H}^{-1}\right|^2 \quad (10)$$

where $k=2\pi/\lambda$ and,

$$\sigma_{1V} = \cos(ka\sin\theta) - j\frac{\sin(ka\sin\theta)}{\sin\theta} \quad (11)$$

$$\sigma_{2V} = \frac{e^{j(ka-\pi/4)}}{\sqrt{2\pi}\,(ka)^{3/2}} \quad (12)$$

$$\sigma_{3V} = \frac{(1+\sin\theta)\,e^{-jka\sin\theta}}{(1-\sin\theta)^2} \quad (13)$$

$$\sigma_{4V} = \frac{(1-\sin\theta)\,e^{jka\sin\theta}}{(1+\sin\theta)^2} \quad (14)$$

$$\sigma_{5V} = 1 - \frac{e^{j(2ka-\pi/2)}}{8\pi(ka)^3} \quad (15)$$

$$\sigma_{1H} = \cos(ka\sin\theta) + j\frac{\sin(ka\sin\theta)}{\sin\theta} \quad (16)$$

$$\sigma_{2H} = \frac{4e^{j(ka+\pi/4)}}{\sqrt{2\pi}\,(ka)^{1/2}} \quad (17)$$

$$\sigma_{3H} = \frac{e^{-jka\sin\theta}}{1-\sin\theta} \quad (18)$$

Eqs. (9) and (10) are valid and quite accurate for aspect angles $0° \le \theta \le 180°$.

The backscattered RCS for a perfectly conducting thin rectangular plate for incident waves at any θ,

$$\sigma_{4H} = \frac{e^{jka\sin\theta}}{1+\sin\theta} \quad (19)$$

$$\sigma_{5H} = 1 - \frac{e^{j(2ka+\pi/2)}}{2\pi(ka)} \quad (20)$$

$$\sigma = \frac{4\pi a^2 b^2}{\lambda}\left[\frac{\sin(ak\sin\theta\cos\phi)}{ak\sin\theta\cos\phi}\,\frac{\sin(bk\sin\theta\sin\phi)}{bk\sin\theta\sin\phi}\right]^2(\cos\theta)^2 \quad (21)$$

ϕ can be expressed by

Eq. (21) is independent of the polarization, and is only valid for aspect angles $\theta \le 20°$

Triangular Flat Plate

Consider the triangular flat plate defined by the

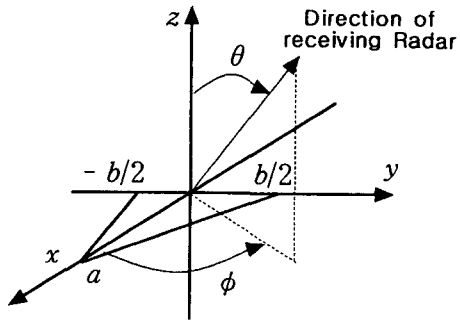

Fig . 4. Coordinates for a isosceles triangular flat plate.

isosceles triangle as oriented in Fig. 4.

The backscattered RCS can be approximated for small aspect angles (less than 20°) by

$$\sigma = \frac{4\pi A^2}{\lambda^2}(\cos\theta)^2\,\sigma_0 \quad (22)$$

$$\sigma_0 = \frac{[(\sin\alpha)^2 - (\sin(\beta/2))^2]^2 + \sigma_{01}}{\alpha^2 - (\beta/2)^2} \quad (23)$$

$$\sigma_{01} = 0.25(\sin\phi)^2[(2a/b)\cos\phi\sin\beta - \sin\phi\sin 2\alpha]^2 \quad (24)$$

where $\alpha = ka\sin\theta\cos\varphi$, $\beta = kb\sin\theta\sin\varphi$, $A = ab/2$.

RCS Calculation of the Three Plates

RCS corresponding to the two Eqs. (7) and (8), the two Eqs. (9) and (21), the Eq. (22) when $\phi = 0$, and the Eq. (22) when $\phi = 90$, are shown in Fig. 5 (a), (b), (c), and (d), respectively. In this cases, let $a=b=r=16.0$cm (5λ) and wavelength

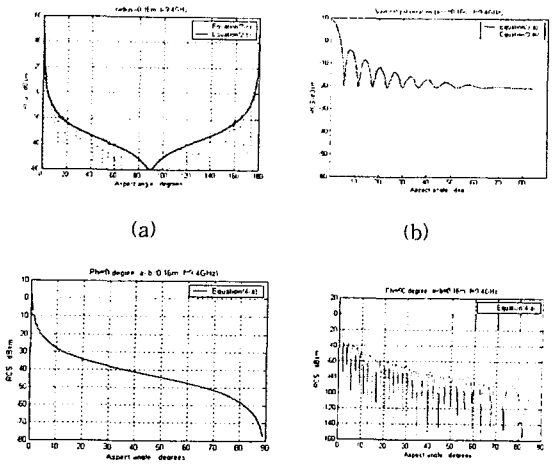

(a) (b)

(c) (d)

Fig . 5 RCS calculation results according to the aspect angle θ and elevation angle ϕ. (a) RCS for a circular flat plate, (b) RCS for a rectangular flat plate, (c) RCS for a (σ v)perfectly conducting triangular flat plate when $\phi=0$, (d) RCS for a perfectly conducting triangular flat plate $\phi=90$

λ = 3.2cm(9.4GHz)

RCS Calculation of Complex shape

A complex target RCS is normally computed by coherently combining the cross sections of the simple shapes that make that target as shown in Figs. (2), (3) and (4). In general, a complex target RCS can be modeled as a group of individual scattering centers distributed over the target. Due to the difficulties associated with the exact RCS prediction for the complex radar target, approximate methods

$$\sigma_{max} = \frac{4\pi a^2}{3\lambda^2} = 4.19\,\frac{a^2}{\lambda^2} \quad (25)$$

$$\sigma_{max} = \frac{16\pi a^2}{3\lambda^2} = 15.61\,\frac{a^2}{\lambda^2} \quad (26)$$

$$\sigma_{max} = \frac{12\pi a^2}{\lambda^2} = 37.67\,\frac{a^2}{\lambda^2} \quad (27)$$

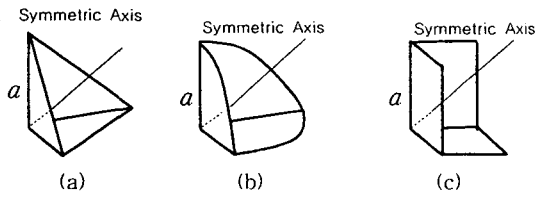

(a) (b) (c)

Fig. 6 Complex radar targets. (a) Triangular tri-hederal type, (b) Circular tri-hederal type, (c) Rectangular tri-hederal type

become the viable alternative.

The following equations are approximated maximum RCS (σ_{max}) at given conditions. Eqs. (25), (26) and (27) correspond to complex targets as shown in Fig.6 (a), (b) and (c), respectively [20]~[25]. Related maximum RCS σ_{Rmax} and related maximum radar detection range, R_{Rmax} , calculated from Eqs. (25), (26) and (27), are summarized as in Table 1.

Table 1 Calculated σ_{Rmax} and R_{Rmax}

Configuration	Related maximum RCS, σ_{Rmax}	Related maximum radar detection range, R_{Rmax}
Triangular tri-hederal	1.0	1.0
Circular tri-hederal	3.7	1.4
Rectangular tri-hederal	8.9	1.7

Selection of Optimum Reflector Shape

In case of the RCS calculation results for the simple targets as shown in Fig. 5, the order of large RCS values at $\theta=0$ is circular flat plat > rectangular flat plat > triangular flat plat, and the order of low RCS degradation speed along with aspect angle θ is rectangular flat plat > circular flat plat > triangular flat plat. In case of the calculation results of related maximum RCS σ_{max} for the complex targets as shown in Table 1, the order of large σ_{max} is rectangular tri-hederal > circular tri-hederal > triangular tri-hederal. Moreover, it is seen that σ_{max} increases very rapidly as radar reflector dimensions are increased since σ_{max} varies as the 4th power of dimension. However, in case of radar detection range R_{Rmax}, increases much more slowly since R_{Rmax} varies directly with radar reflector dimensions. Thus, doubling the size of the radar reflector will not usually double the detection range.

The important fact in reflector design is that the rectangular flat plat is seldom used in marine systems due to its non-compatibility with sails and rigging, and also due to its extra weight and high vulnerability to windage. Thus, circular tri-hederal type was used in the development of PRR-S-

TAGS, in this paper.

4. PRR-S MODELING

4.1 Design Concepts

A professional radar reflector produces a much stronger return of the radar signal than might be expected by its modest dimensions. The conventional radar reflector consists of three mutually perpendicular metal plates which form 8 individual corners, or pockets. If one of these pockets were to be placed on a flat surface, a line rising perpendicularly from the flat surface to the peaked junction of the three sides of the plates would be called the 'axis of symmetry' as shown in Fig. 6. The inner sides of the pocket, which form the corners of the reflector, have the unique property of always reflecting the radar signal back to its originating source with high levels of effectiveness over angles that vary from the 'axis of symmetry' by 20° or more.

In the 'catch rain' position optimum 360° azimuth coverage is provided, and at the same time, the pocket pointing straight up will aid in airborne search and rescue operations. Because of the importance of using the correct orientation of the reflector, and to achieve maximum detection probability, PRR-S is modeled with a three-axis gimbaled stabilizer to assure that the correct 'catch rain' position even ship's heeling.

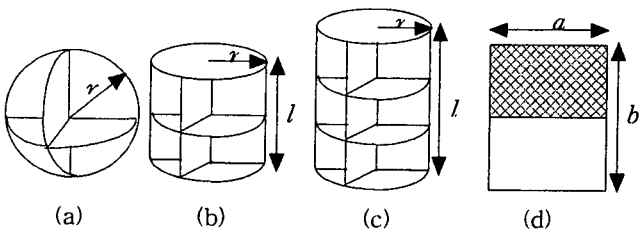

Fig. 7 PRR-S Models of octahederal-type reflectors. (a) Sphere-type, (b) Cylinder-type, (c) Double cylinder-type, (c) Radar flag

Table 2 Dimensions of octahederal-type reflectors

No.	Type	Material	r (cm)	l (cm)	a(cm)	b(cm)
1	Sphere	Aluminum	7.5	-	-	-
2	Sphere	Bronze	7.5	-	-	-
3	Sphere	Aluminum	15.0	-	-	-
4	Sphere	Bronze	15.0	-	-	-
5	Cylinder	Aluminum	7.5	15.0	-	-
6	Cylinder	Bronze	7.5	15.0	-	-
7	Double-cylinder	Aluminum	7.5	22.5	-	-
8	Double-cylinder	Bronze	7.5	22.5	-	-
9	Cylinder	Aluminum	15.0	30.0	-	-
10	Cylinder	Bronze	15.0	30.0	-	-
11	Double-cylinder	Aluminum	15.0	45.0	-	-
12	Double-cylinder	Bronze	15.0	45.0	-	-

4.2 Construction of PRR-S

PRR-S is consists of octahederal-type reflector and three-axis gimbal. Fig. 7 shows the four kinds of

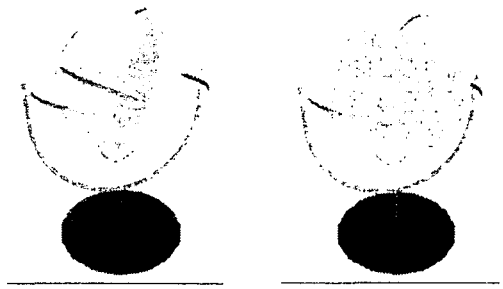

(a) (b)

Fig. 8 Three-dimensional Virtual Reality models of the PRR-S assembled with three-axis gimbaled stabilizer. (a) In case of Sphere-type, (b) in case of Cylinder-type

modeled octahederal-type reflectors only. Where, the Fig. 7(a), (b) and (c) are metal reflectors, while the Fig. 7(d) is radar flag fabricated with nylon and steel nets. Their dimensions are represent in Table 2.

4.3 Test Results of PRR-S

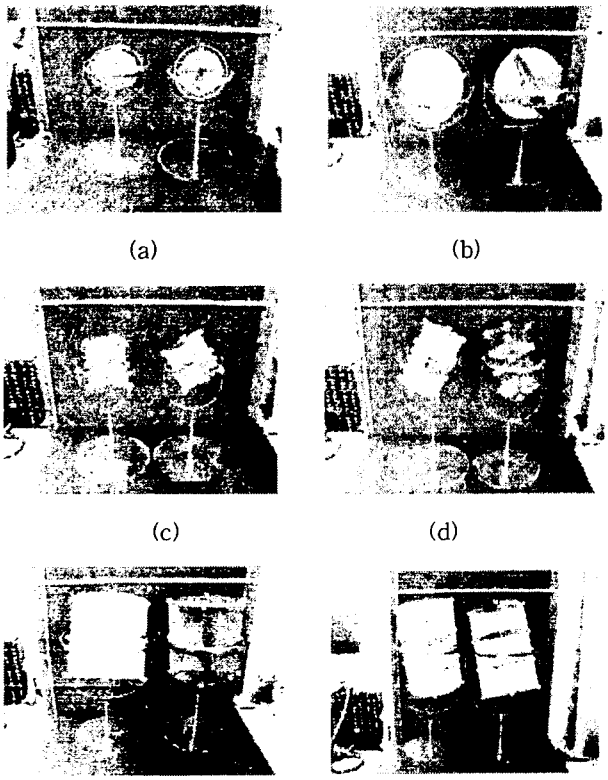

(a) (b)

(c) (d)

(e) (f)

Fig. 9 Photographs of the end structure of PRR-S. (a) No.1 and No.2, (b) No.3 and No.4, (c) No.5 and No.6, (d) No.7 and No.8, (e) No.9 and No.10, (f) No.11 and No.12. Where the 'No.' denotes reflector numbers as shown in Table 2.

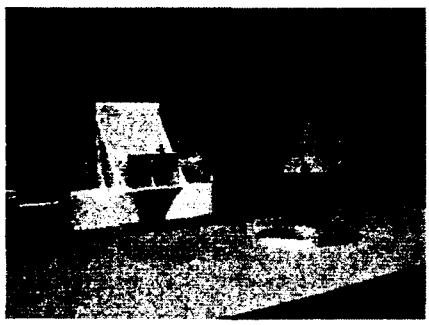

Fig. 10 Test environment

Performance tests for the PRR-S are carried out in an anechoic chamber of Korea Maritime University in Korea. Fig. 10 shows test environment in the anechoic chamber. RCS test results

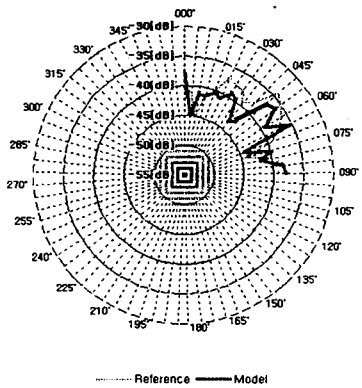

(a) Sphere, Aluminum, r=15cm, l=30cm

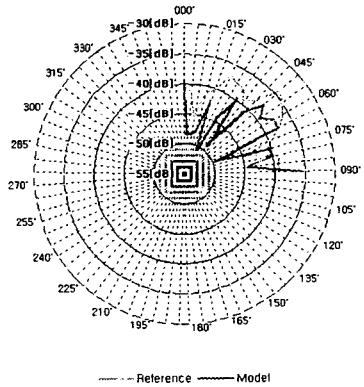

(b) Sphere, Bronze, r=15cm, l=30cm

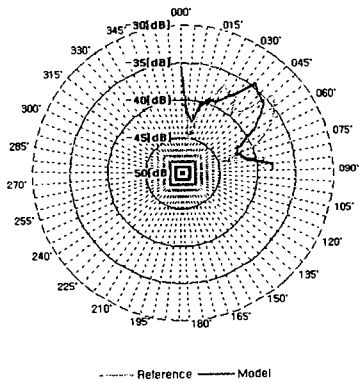

(c) Double Cylinder, Aluminum, r=15cm, l=30cm

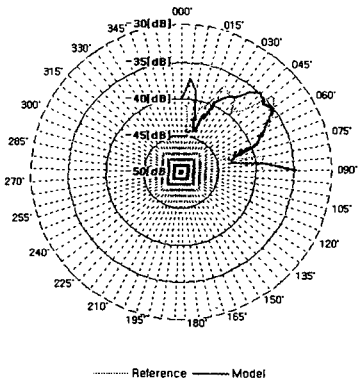

(d) Double Cylinder, Bronze, r=15cm, l=30cm

Fig. 11 RCS test results

represented in Fig. 11

RCS test results show that the RCS value of PRR-S is more large than the reference reflector (Davis Echomaster).

Since more detailed RCS tests are under proceeding in now, full of RCS polar plot and dynamic behavior of gimbaled stabilizer are not shown in this paper. That results will be present next seminar.

5. CONCLUSIONS

A new Passive-type Radar Reflector (PRR-S) is designed in this study. Through the analysis of simple and complex radar targets, optimum shape of reflector plate can be obtained. As RCS test results, it is shown that the PRR-S gives more high performence than the model radar reflector (Davis Echomaster).

◈ REFERENCES ◈

[1] Jeong-Bin Yim, H.R. Kim, K.D. Lee, "Research on the Required Specifications for the Ship's Sound Reproduction System According to SOLAS 2000," Proc. of Summer Meeting 2002, Acoustical Society of Korea, Vol.21, No.1(s), pp. 411-414, 2002.5.6.

[2] Woo-Suck Kim, Y.S. Ahn, I H. Kim, J.B. Yim, S.H. Park, "A Development of RADAR Reflector for Fishing Net Buoy," Proc. of the 26th Annual Spring Meeting on Navigation and Port Research 2002, Korean Institute of Navigation and Port Research, pp.177-184, 2002.3.29

[3] Seong-Hyen Park, W.S. Kim, Y.S. Ahn, I.H. Kim, J.B. Yim, "Study on the Dynamic Response Analysis of the Barge Type Offshore Structure for Fishery, Proc. of the 26th Annual Spring Meeting on Navigation and Port Research, 2002, Korean Institute of Navigation and Port Research, pp.155-160, 2002.3.29

[4]. Davis, Davis Echomaster & Emergency, URL://www.davisnet.com.

[5]. Landfall Navigation, Firedell Blipper Reflector, URL://www.landfallnavigation.com.

[6]. Landfall Navigation, Mobri Cylindrical Radar Reflector, URL://www.landfallnavigation.com.

[7]. North Sea Navigator, Inc, Cyclops Models and Specifications, URL://www.northseanavigator.com.

[8]. Tri-lens Inc., The Tri-Lens Radar Reflector, URL://www.tri-lens.com.

[9]. Radar Flag, Radar flag, URL://www.ladarflag.com.

[10] Jeong-Bin Yim, W.S. Kim, Y.S. Ahn, I.H. Kim, S.H. Park "A Study on the RCS Enhancement Method of Passive RADAR Reflector Through Shaping," Proc. of the 26th Annual Spring Meeting on Navigation and Port Research 2002, Korean Institute of Navigation and Port Research, pp.161-176, 2002.3.29

[11] Jeong-Bin Yim, W.S. Kim, Y.S. Ahn, I.H. Kim, S.H. Park, "Development Techniques on the Radar Reflector, Proc. of the Annual Spring Meeting on Maritime Industry, Institute of Maritime Industry, 2002.4.20

[12]. IMO, Sub-Committee on Safety of Navigation 46th Session, Report to the Maritime Safety Committee, Annex 20: Draft Amendments to Chapter 13 of the HSC Code, 2000, 2000.7.

[13]. IMO 10th Session, Resolution A.384(Ⅹ), Performance Standards for Radar Reflectors, Adopted on 14 November 1977.

[14]. IMO 8th Session, Resolution A.277(Ⅷ), Recommendation on Performance Standards for Radar Reflectors, Adopted on 20 November 1973.

[15]. Eugene F. Knott, Radar Cross Section Measurement, Van Nostrand Reinhold, 1993, pp.1-26.

[16]. Jim Coreman, Chuck Hawley, Dick Honey and Stan Honey, 1995 Radar Reflector Test, URL://www.ussailing.org.

[17]. Merrill L. Skolnik, Introduction to Radar Systems, McGraw Hill, 2001, pp.30-98.

[18]. Bassem R. Mahafza, Radar Systems Analysis and Design Using MATLAB. Champman & Hall/CRC, 2000, pp.71-140.

[19]. Asoke K. Bhattacharyya, and D.L. Sengupta, Radar Cross Section Analysis & Control, Artech House, 1991, pp.1-140.

[20]. Smi Fifth Annual Event, RCS Modeling and Analysis, 2001.8, URL://www.naval-technology.com.

[21]. CSSDENMARK, Radar Cross Section Simulation Software for Stealth Assessment, URL://www.naval-technology.com.

[22]. National Institute of Standard Technology, Metrology for Radar Cross Section Systems, URL://www.boulder.nist.gov.

[23]. Ohio University, Current Reaseach: Compact Radar Measurement Range, URL://esl.eng.ohio-state.edu.

[24]. Ohio University, Antenna/RCS Measurement Workshop, June, 2001, URL://esl.eng.ohio-state.edu.

[25]. Rozendal Associates, Radar Reflectors, URL//www.strandnet.com.

[26] Jeong-Bin Yim, H.R. Kim, K.D. Lee, "A Study on the Creation of Stereoscopic Image and Three-Dimensional Sound in a Virtual Space," Proc. of Summer Meeting 2002, Acoustical Society of Korea, Vol.21, No.1(s), pp. 399-402, 2002.5.6